Electronic Supplementary Information

NASICON vs. Na Metal: A New Counter Electrode to Evaluate Electrodes for Na Secondary Batteries

Jinkwang Hwang,[a] Koki Takeuchi ,[a]Kazuhiko Matsumoto,*[,a,b] Rika Hagiwara[a,b]

[a] Graduate School of Energy Science, Kyoto University, Sakyo-ku, Kyoto 606-8501, Japan
E-mail: k-matsumoto@energy.kyoto-u.ac.jp

[b] Unit of Elements Strategy Initiative for Catalysts & Batteries (ESICB), Kyoto University, Katsura, Kyoto 615-8510, Japan

*Corresponding author: Kazuhiko Matsumoto
E-mail: k-matsumoto@energy.kyoto-u.ac.jp
Tel: +81757534817
Fax: +81757535906

1. Additional comments on the data in supplementary information

Structures of $Na_3V_2(PO_4)_3$ and $NaV_2(PO_4)_3$

Fig. S1 and S2 show the refined crystal structure models of the prepared $Na_3V_2(PO_4)_3$ and $NaV_2(PO_4)_3$, respectively (see Fig. 2 for the XRD data and Tables S1 and S2 for the crystallographic data). The constituent Na ions selectively occupy two distinct sites labeled as Na1 (occupancy of 0.7656) and Na2 (occupancy of 0.7488) sites in $Na_3V_2(PO_4)_3$. After desodiation by Cl_2 gas along with the redox activity from V^{3+} to V^{4+}, the occupancies of Na1 and Na2 change to 0.954 and 0, suggesting Na ions were desodiated from Na2 site and some of them migrated to Na1 site. The same trend was reported in the electrochemical desodiation of $Na_3V_2(PO_4)_3$ to $NaV_2(PO_4)_3$ in the previous study.[1]

Electrochemical performance

Fig. S3, S4, and S5 show the rate performance of the Na/IL/$Na_3V_2(PO_4)_3$, Na/IL/ $NaV_2(PO_4)_3$, and Na/IL/N_3N_1VP cells at 90 ºC, respectively. The cell was charged up to 3.6 V at 1C and discharged at 1 to 100C for 3 cycles at each current density. The characteristic flat plateau was maintained even at a very high current density because elevation of temperature improved the interfacial process and ion transport, as previously reported.[2, 3] Fig. S6, S7, and S8 show the rate performance of N_3N_1VP/N_3N_1VP symmetric cell using OE at 25 ºC and IL at 25 and 90 ºC. The flat plateau and small polarization were maintained up to 10 C for OE at 25 ºC (Fig. S6), whereas they were maintained up to 5 C for IL at 25 ºC (Fig. S7) and 20 C for IL at 90 ºC (Fig. S8).

Cyclic voltammetric (CV) studies of the N_3N_1VP/Al cells were performed to examine the electrochemical window of the OE and IL electrolytes (Fig. S10). The cells were scanned

with 1 mV s^{-1} and showed the excellent stability of Al current collector with the N_3N_1VP counter electrode in OE and IL electrolytes. The CV results suggested the validity of N_3N_1VP for a counter electrode to test another electrode and electrolyte materials for sodium secondary batteries in the electrochemical window of −3.4 to 2 V vs. N_3N_1VP (corresponding to 0.0 to 5.4 V vs. Na/Na^+).

Fig. S11 shows charge-discharge curves of the $Na/OE/Na_3V_2(PO_4)_3$ cell and $N_3N_1VP/OE/Na_3V_2(PO_4)_3$ cell at 25 ºC. As shown in Fig. S11a, the $Na/OE/Na_3V_2(PO_4)_3$ cell is unstable in the initial cycles, which is consistent with a previous report,[4] due to the instability properties of Na metal counter electrode and OE as explained in the main text for the $Na/OE/Na_2FeP_2O_7$ cell (Fig. 5). Such instability was not observed for the $N_3N_1VP/OE/Na_3V_2(PO_4)_3$ cell or the cells with the IL electrolyte (Fig. S11b and S12). Similar electrochemical behavior was observed for the $NaCrO_2$ positive electrode (Fig. S14 and S15).

2. Additional information on experimental section

Material characterization

X-ray diffraction patterns were collected in the Bragg-Brentano geometry (40 kV and 30 mA) and with a silicon strip high-speed detector (Rigaku D/teX Ultra 250) using a Rigaku SmartLab diffractometer. X-ray diffraction patterns were analyzed by the Rietveld refinement using the FullProf software.[5] The resulting crystal structures were drawn using the VESTA program.[6] The synthesized samples were observed by scanning electron microscopy (Hitachi SU-8020). The element composition of the samples was obtained by energy dispersive X-ray analysis (Horiba EMAXEvolution X-max).

Electrochemical measurement

Electrochemical properties were measured using 2032 coin-type cells. The cells were assembled under dry Ar atmosphere. Charge-discharge properties, rate capabilities, and cycling were evaluated using an HJ1001SD8 charge-discharge test device (Hokuto Denko). All electrochemical measurements were started 3-hour after the relevant temperature adjustments. Measurements were carried out using a VSP potentiostat (Bio-Logic) over a frequency range from 10 mHz−100 kHz with a perturbation amplitude of 10 mV or 100 μA.

Preparation of Hard Carbon Negative Electrode

A slurry was prepared by mixing hard carbon powders (CARBOTRON P, Kureha Battery Materials Japan Co., Ltd.), carbon black and PVDF (85:5:10 wt%) in N-methylpyrrolidone using a planetary mixer (AR-100, Thinky, Tokyo, Japan) and pasting the mixture on an Al foil. The electrodes were dried at 353 K for 12 h

Table S1 Structural parameters of $Na_3V_2(PO_4)_3$ from the Rietveld refinement of XRD patterns

$Na_3V_2(PO_4)_3$ (S.G. $R\bar{3}c$)
R_p = 11.1%, R_{wp} = 12.8%, R_e = 3.5, a = 8.7305(1) Å, c = 21.858(4) Å

Atom	Wyckoff symbol	x	y	z	B_{iso}/Å^2	Occup.
Na1	6b	0	0	0	0.5	0.7656(8)
Na2	18e	0.6315(8)	0	0.2500	0.5	0.7488(5)
V	12c	0	0	0.1509(1)	0.5	1.000
P	18e	0.2942(1)	0	0.2500	0.5	1.000
O1	36f	0.1920(8)	0.9664(4)	0.1948(5)	0.5	1.000
O2	36f	0.1857(3)	0.1523(9)	0.0905(0)	0.5	1.000

Table S2 Structural parameters of $NaV_2(PO_4)_3$ from the Rietveld refinement of XRD patterns.

$NaV_2(PO_4)_3$ (S.G. $R\bar{3}c$) R_p = 12.6%, R_{wp} = 10.6%, R_e = 6.1, a = 8.4335(5) Å, c = 21.543(1) Å						
Atom	Wyckoff symbol	x	y	z	B_{iso}/Å^2	Occup.
Na	6b	0	0	0	0.5	0.954(1)
V	12c	0	0	0.1445(6)	0.5	1.000
P	18e	0.3076(2)	0	0.2500	0.5	1.000
O1	36f	0.1556(4)	0.9987(1)	0.1788(2)	0.5	1.000
O2	36f	0.2433(4)	0.1518(1)	0.0657(2)	0.5	1.000

Table S3 Results of energy dispersive X-ray spectroscopic analysis on $Na_3V_2(PO_4)_3$ and $NaV_2(PO_4)_3$.[a]

Atoms	V		P		Na	
	Obs. / %	Calc. / %	Obs. / %	Calc. / %	Obs. / %	Calc. / %
$Na_3V_2(PO_4)_3$	23.2	22.4	20.8	20.4	14.5	15.1
$NaV_2(PO_4)_3$	23.9	24.8	23.9	22.7	6.2	5.6

[a]The amount of carbon was omitted from the calculation of elemental composition by weight. Carbon content of $Na_3V_2(PO_4)_3$ and $NaV_2(PO_4)_3$ are 10% and 12 % according to combustion analysis.

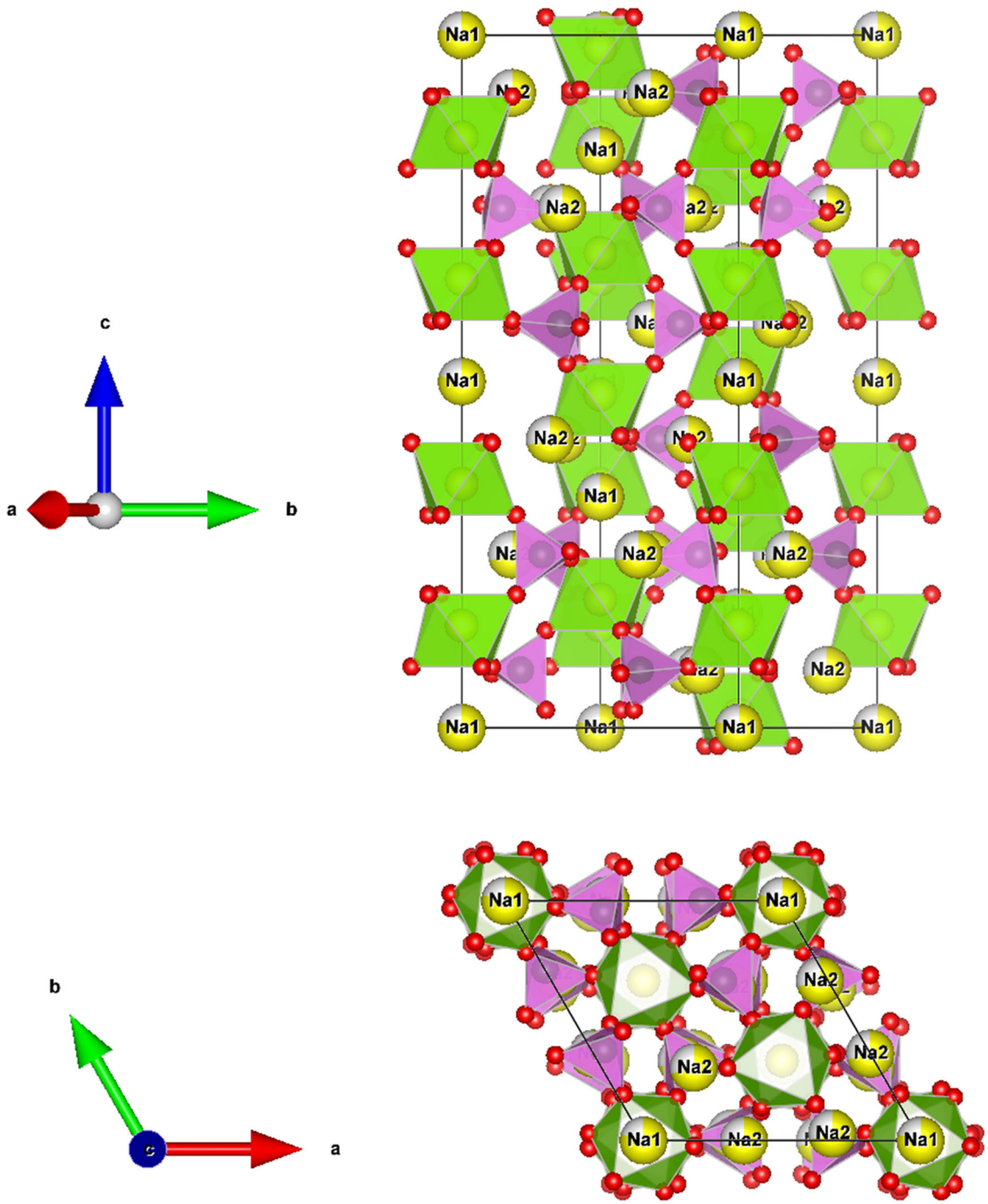

Fig. S1 Refined crystal structure of $Na_3V_2(PO_4)_3$; yellow, red, green, and purple denote Na, O, VO_6, and PO_4, respectively.

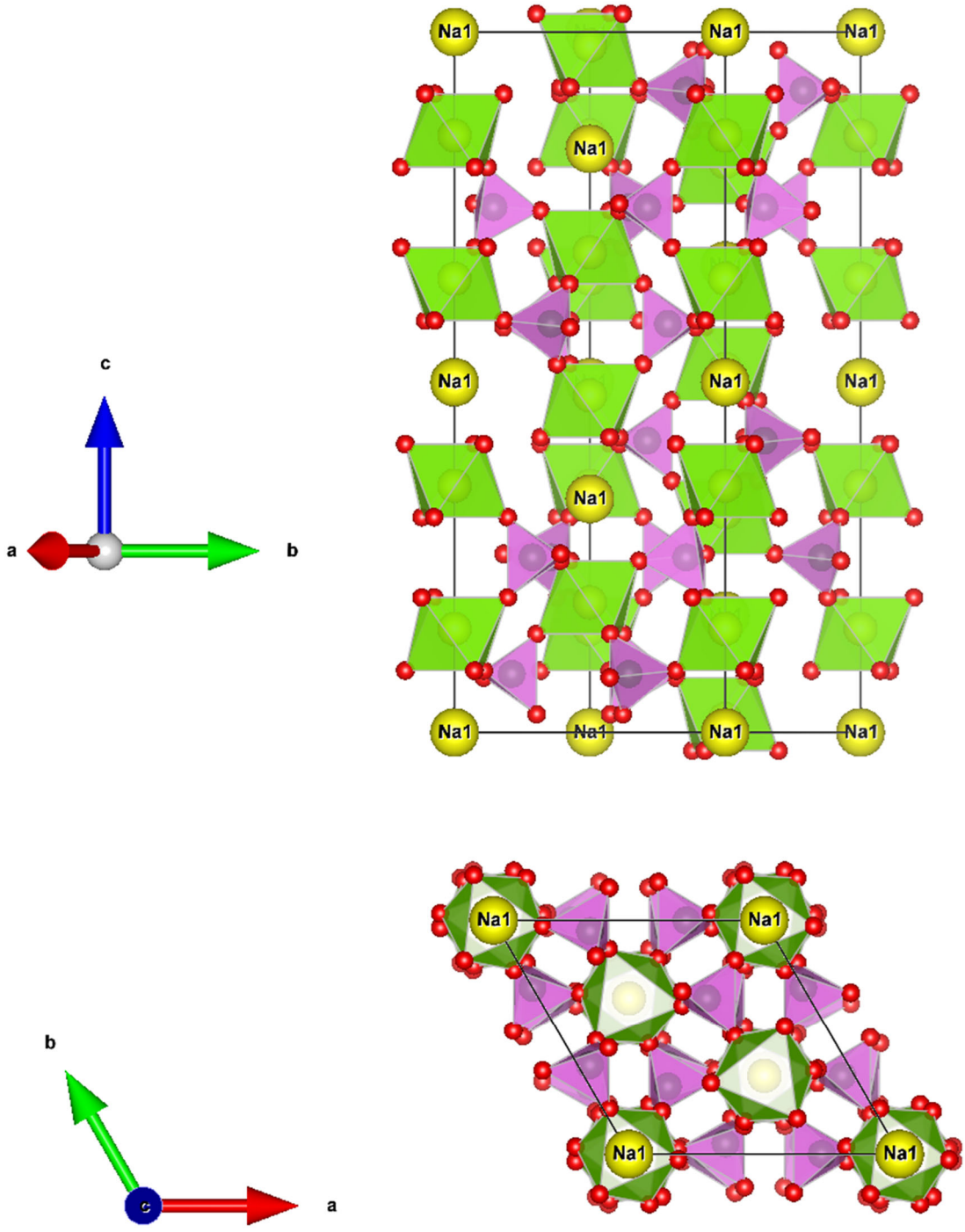

Fig. S2 Refined crystal structure of $NaV_2(PO_4)_3$: yellow, red, green, and purple denote Na, O, VO_6, and PO_4, respectively.

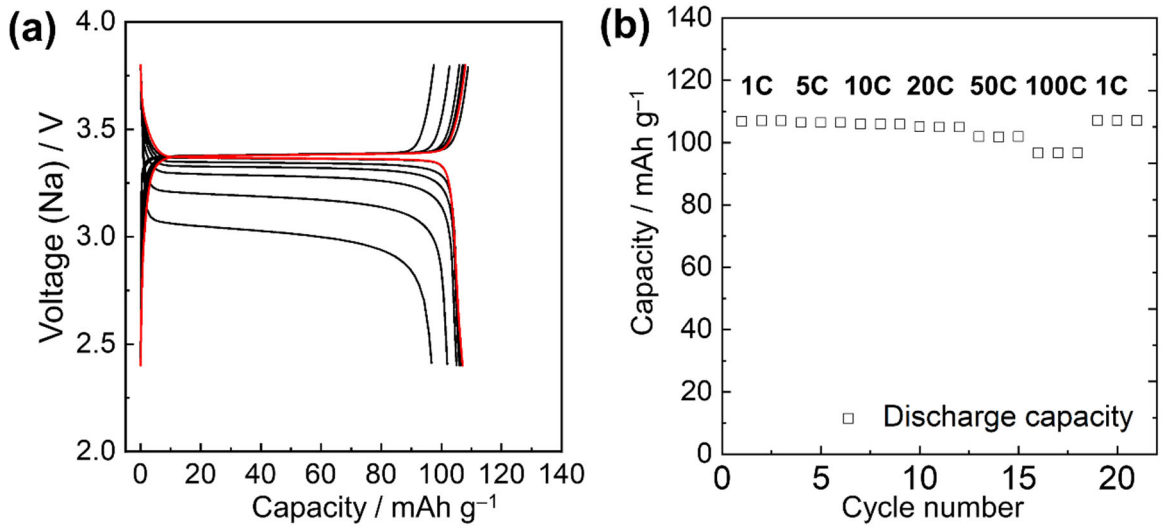

Fig. S3 Rate capability of the Na/IL/$Na_3V_2(PO_4)_3$ cell at 90 ºC. a) Charge-discharge curves. Red curves refer to the discharge profile at 1C after the rate capability test up to 100C. b) Rate capability plots. C-rate: 1C for charge and 1−100C for discharge. Cutoff voltage: 2.4/3.8 V.

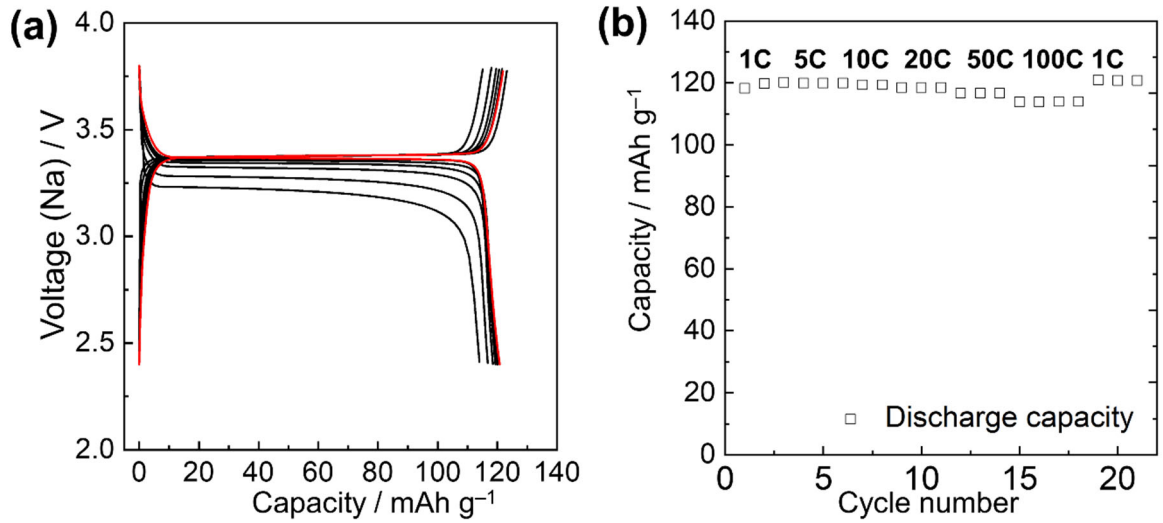

Fig. S4 Rate capability of the Na/IL/$NaV_2(PO_4)_3$ cell at 90 ºC. a) Charge-discharge curves. Red curves refer to the discharge profile at 1C after the rate capability test up to 100C. b) Rate capability plots. C-rate: 1C for charge and 1−100C for discharge. Cutoff voltage: 2.4/3.8 V.

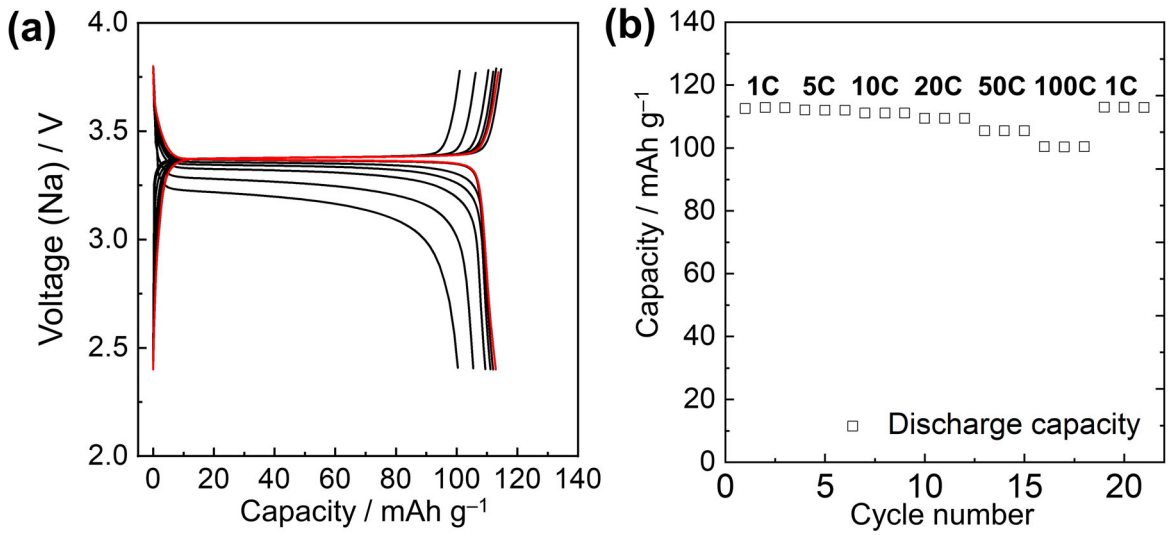

Fig. S5 Rate capability of the Na/IL/N_3N_1VP cell at 90 ºC. a) Charge-discharge curves. Red curves refer to the discharge profile at 1C after the rate capability test up to 100C. b) Rate capability plots. C-rate: 1−100C for discharge. Cutoff voltage: 2.4/3.8 V.

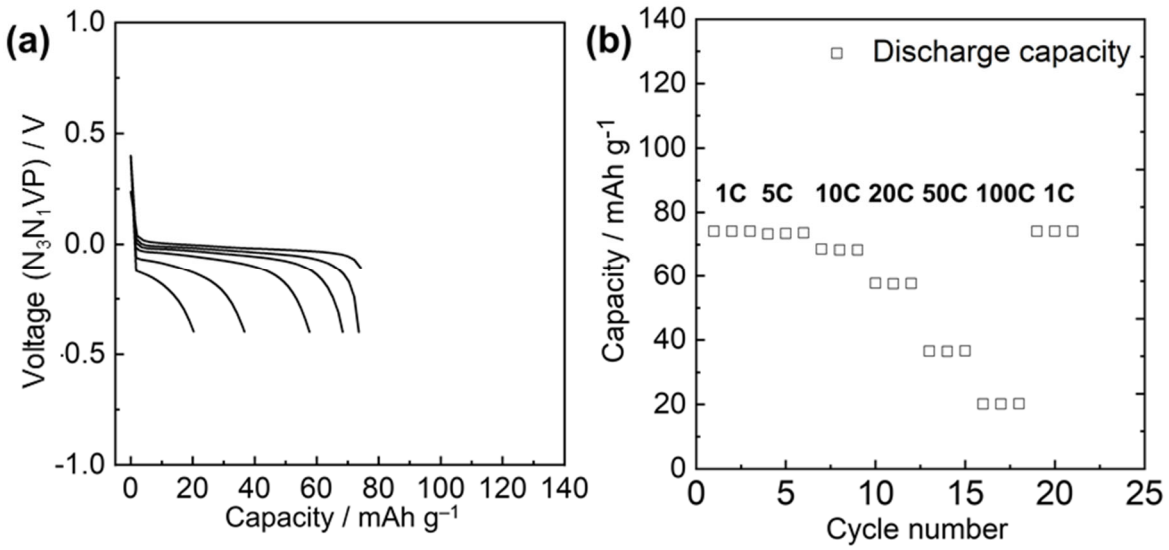

Fig. S6 Rate capability of the N_3N_1VP/OE/N_3N_1VP symmetric cell at 25 ºC. a) Discharge curves. b) Rate capability plots. C-rate: 1−100C. Cutoff voltage: –0.4/0.4 V. The charge-discharge capacity is restricted to 70% in this test by measurement time and cut-off voltage.

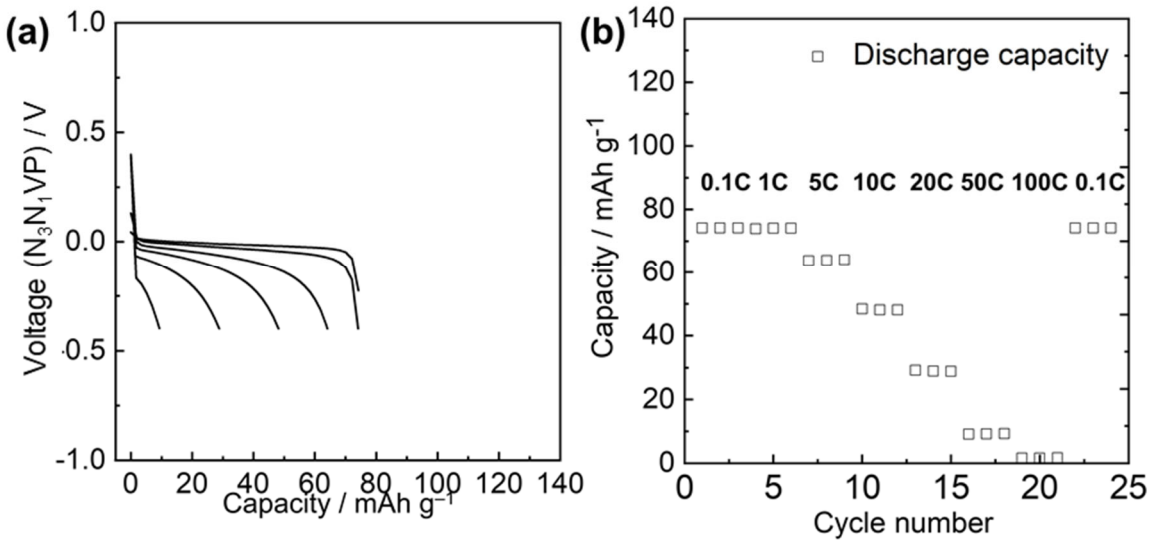

Fig. S7 Rate capability of the N_3N_1VP/IL/N_3N_1VP symmetric cell at 25 ºC. a) Discharge curves. b) Rate capability plots. C-rate: 1−100C. Cutoff voltage: –0.4/0.4 V. The charge-discharge capacity is restricted to 70% in this test by measurement time and cut-off voltage.

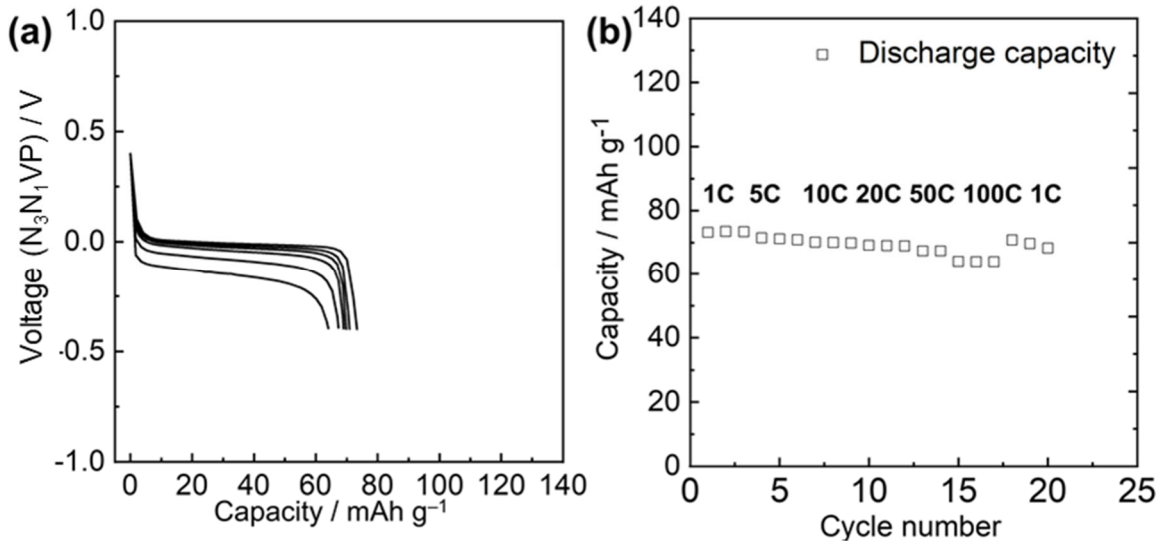

Fig. S8 Rate capability of the N_3N_1VP/IL/N_3N_1VP symmetric cell at 90 ºC. a) Discharge curves. b) Rate capability plots. C-rate: 1−100C. Cutoff voltage: –0.4/0.4 V. The charge-discharge capacity is restricted to 70% in this test by measurement time and cut-off voltage.

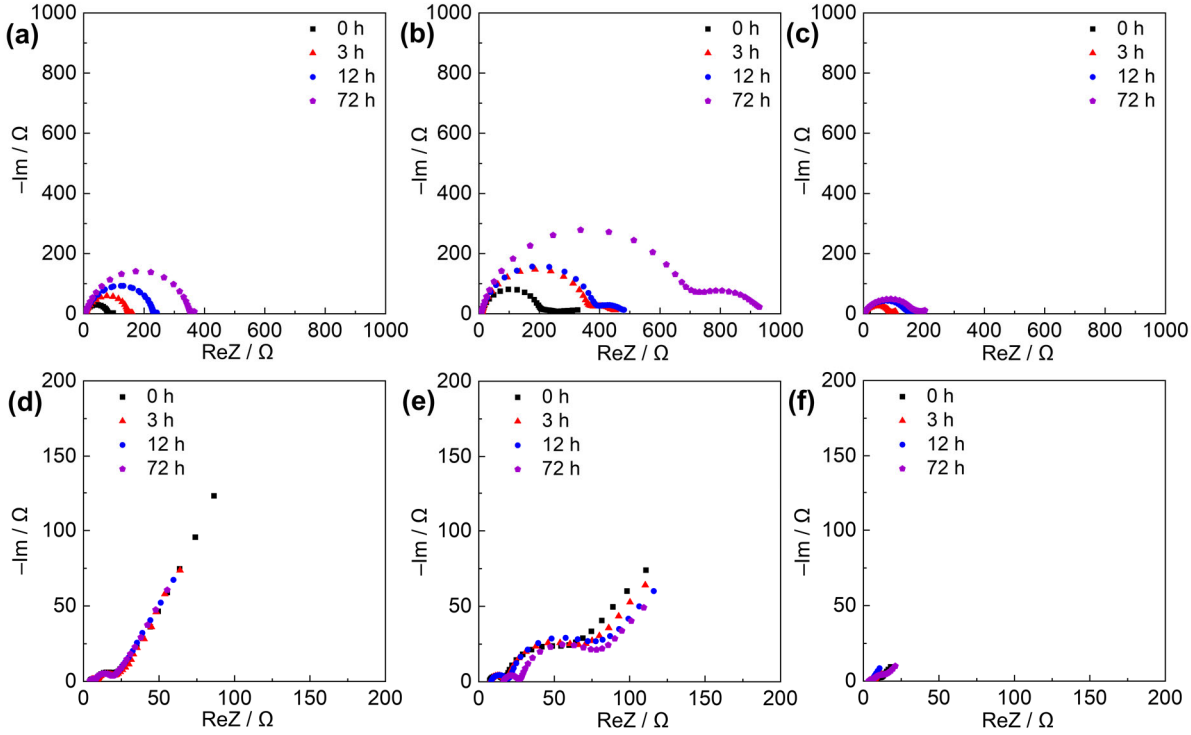

Fig. S9 Time dependence of Nyquist plots for the symmetric cells. a) Na/OE/Na cell at 25 ºC, b) Na/IL/Na cells at 25 ºC, c) Na/IL/Na cell at 90 ºC, d) N_3N_1VP/OE/N_3N_1VP cell at 25 ºC, e) N_3N_1VP/IL/N_3N_1VP cell at 25 ºC, and f) N_3N_1VP/IL/ N_3N_1VP cell at 90 ºC. Frequency range: 10 mHz−100 kHz.

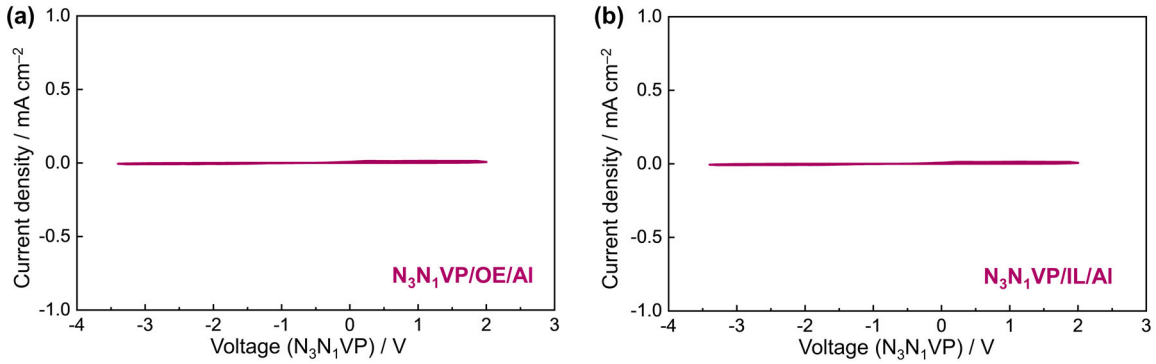

Fig. S10 Cyclic voltammograms of the N_3N_1VP/Al cell in (a) OE and (b) IL electrolytes at 25 ºC. Scan rate: 1 mV s^{-1}.

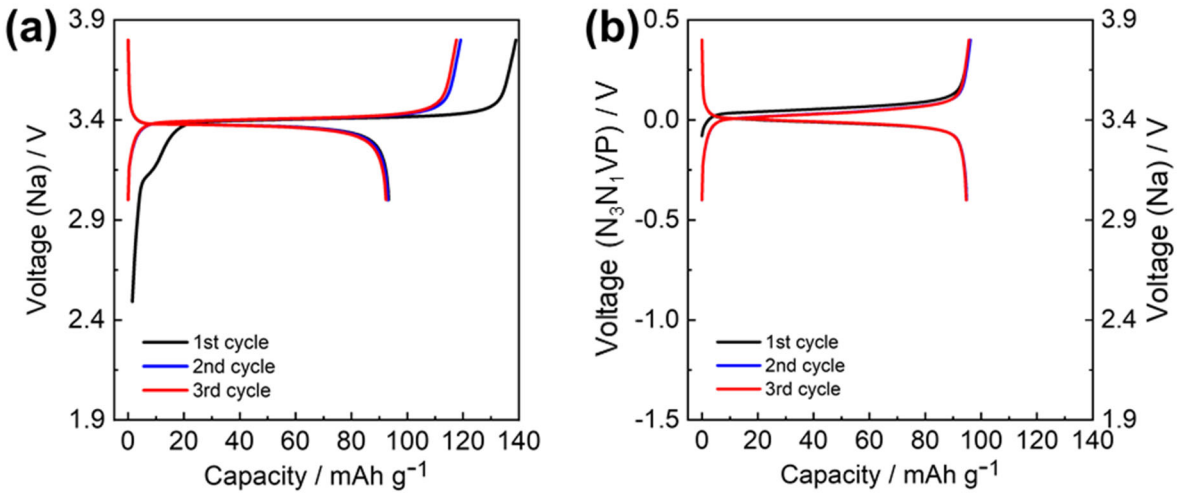

Fig. S11 Charge-discharge curves of the a) Na/OE/$Na_3V_2(PO_4)_3$ cell and b) N_3N_1VP/OE/$Na_3V_2(PO_4)_3$ cell at 25 ºC. C-rate: 1C. Cutoff voltage: 2.4/3.8 V for Na/OE/$Na_3V_2(PO_4)_3$ cell and –0.4/0.4 V for N_3N_1VP/OE/$Na_3V_2(PO_4)_3$ cells.

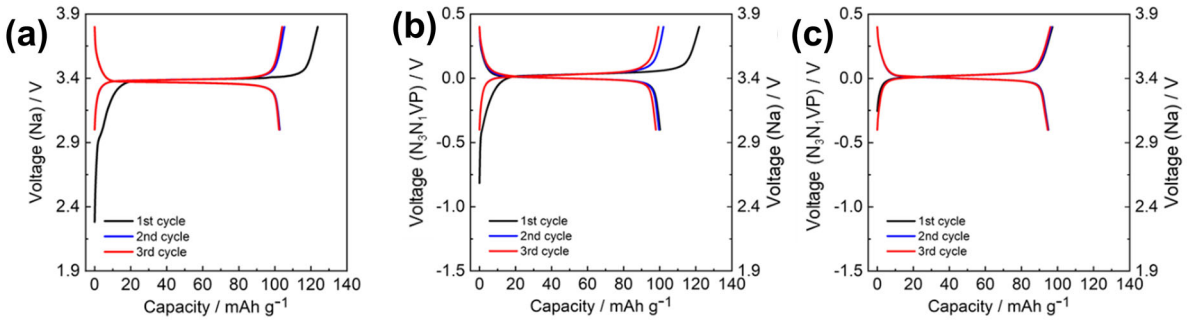

Fig. S12 Charge-discharge curves of the a) Na/IL/$Na_3V_2(PO_4)_3$ cell at 90 ºC, b) N_3N_1VP/IL/$Na_3V_2(PO_4)_3$ cell at 90 ºC, and c) N_3N_1VP/IL/$Na_3V_2(PO_4)_3$ cell at 110 ºC. Current densities: 1C. Cutoff voltage: 2.4/3.8 V for the Na/IL/$Na_3V_2(PO_4)_3$ cell and –0.4/0.4 V for N_3N_1VP/IL/$Na_3V_2(PO_4)_3$ cells. The cell at 110 ºC was charge-discharged after cycling at lower temperatures.

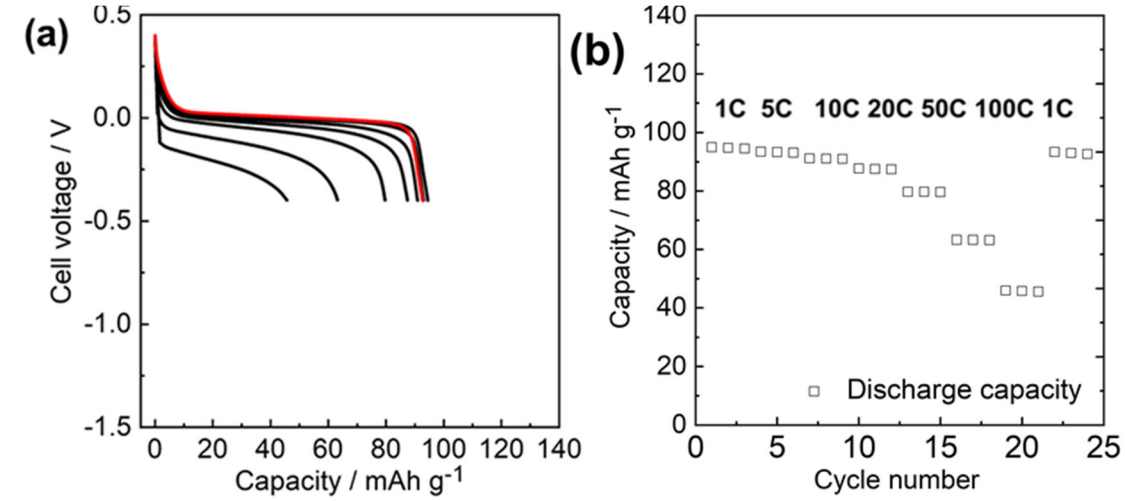

Fig. S13 Rate capability of the $N_3N_1VP/IL/Na_3V_2(PO_4)_3$ cell. a) discharge curves at 110 ºC and b) rate capability plots at 110 ºC. Red curves refer to the discharge profile at 1C after the rate capability test up to 100C. Current densities: 1−100C. Cutoff voltage: –0.4/0.4 V.

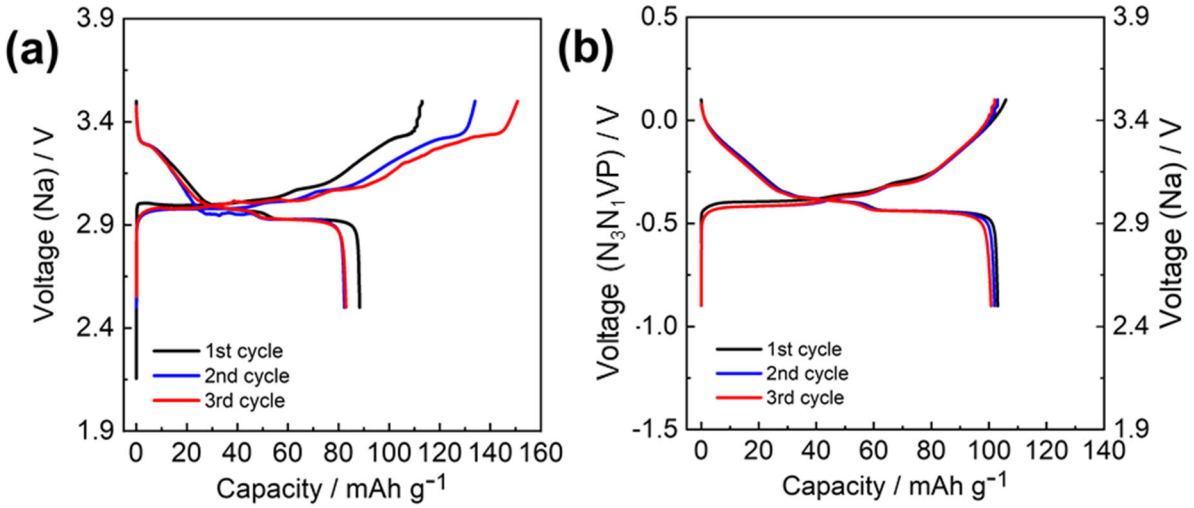

Fig. S14 Charge-discharge curves of the a) Na/OE/$NaCrO_2$ cell and b) N_3N_1VP/OE/ $NaCrO_2$ cell at 25 ºC. Current densities: 1C. Cutoff voltage: 2.5/3.5 V for the Na/OE/$NaCrO_2$ cell and –0.9/0.1 V for the N_3N_1VP/OE/$NaCrO_2$ cell.

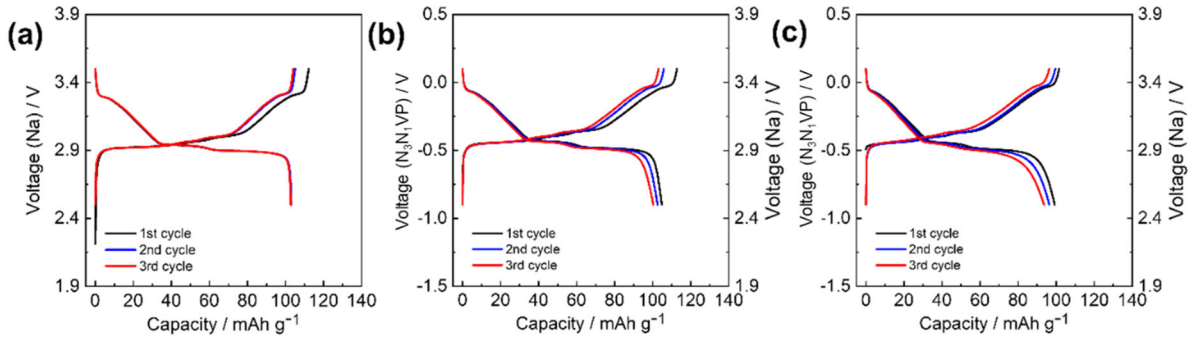

Fig. S15 Charge-discharge curves of the a) Na/IL/$NaCrO_2$ cell at 90 ºC, b) N_3N_1VP/IL/ $NaCrO_2$ cell at 90 ºC, c) N_3N_1VP/IL/$NaCrO_2$ cell at 110 ºC Current densities: 1C. Cutoff voltage: 2.5/3.5 V for the Na/IL/$NaCrO_2$ cell and –0.9/0.1 V for the N_3N_1VP/IL/$NaCrO_2$ cells.

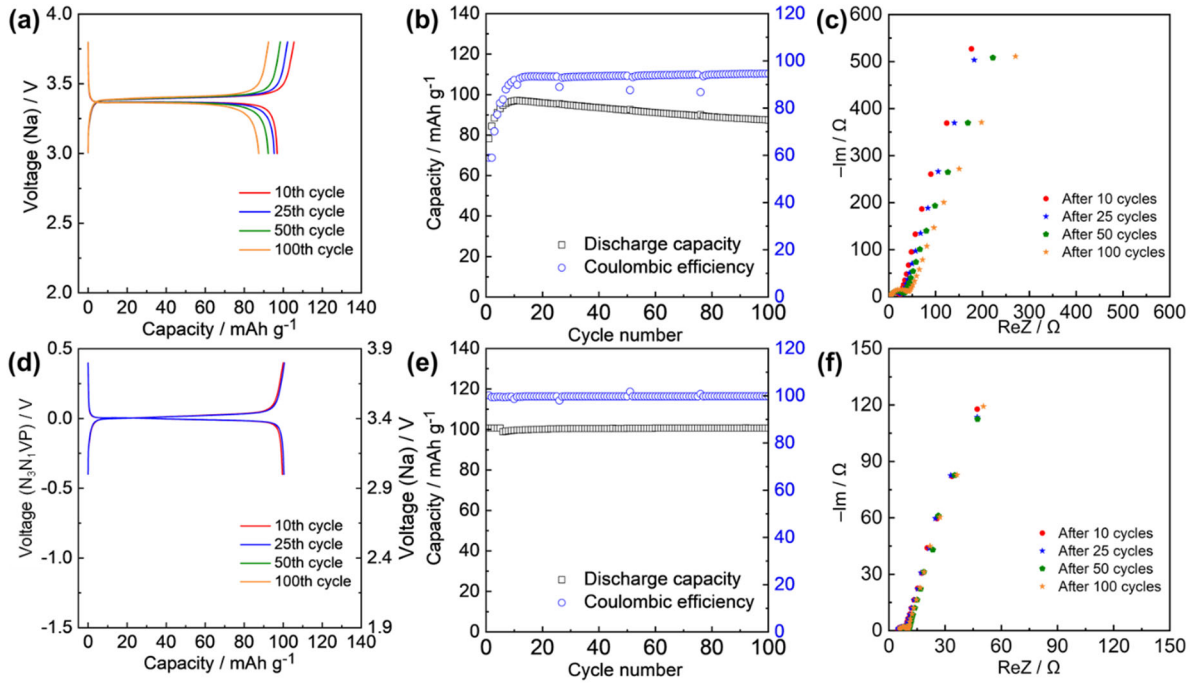

Fig. S16 Cycling performance and the corresponding Nyquist plots at 25 ºC for the cells with the $Na_3V_2PO_4$ working electrode. a) Charge-discharge curves, b) cycling plots, and c) Nyquist plots of the Na/OE/$Na_3V_2(PO_4)_3$ cell. d) Charge-discharge curves, cycling plots, and Nyquist plots of the N_3N_1VP/OE/$Na_3V_2(PO_4)_3$ cell. Rate: 1C. Cutoff voltage: 3.0/3.8 V for the Na/OE/$Na_3V_2PO_4$ cell and –0.4/0.4 V for the N_3N_1VP/OE/$Na_3V_2(PO_4)_3$ cell. Frequency range: 10 mHz−100 kHz.

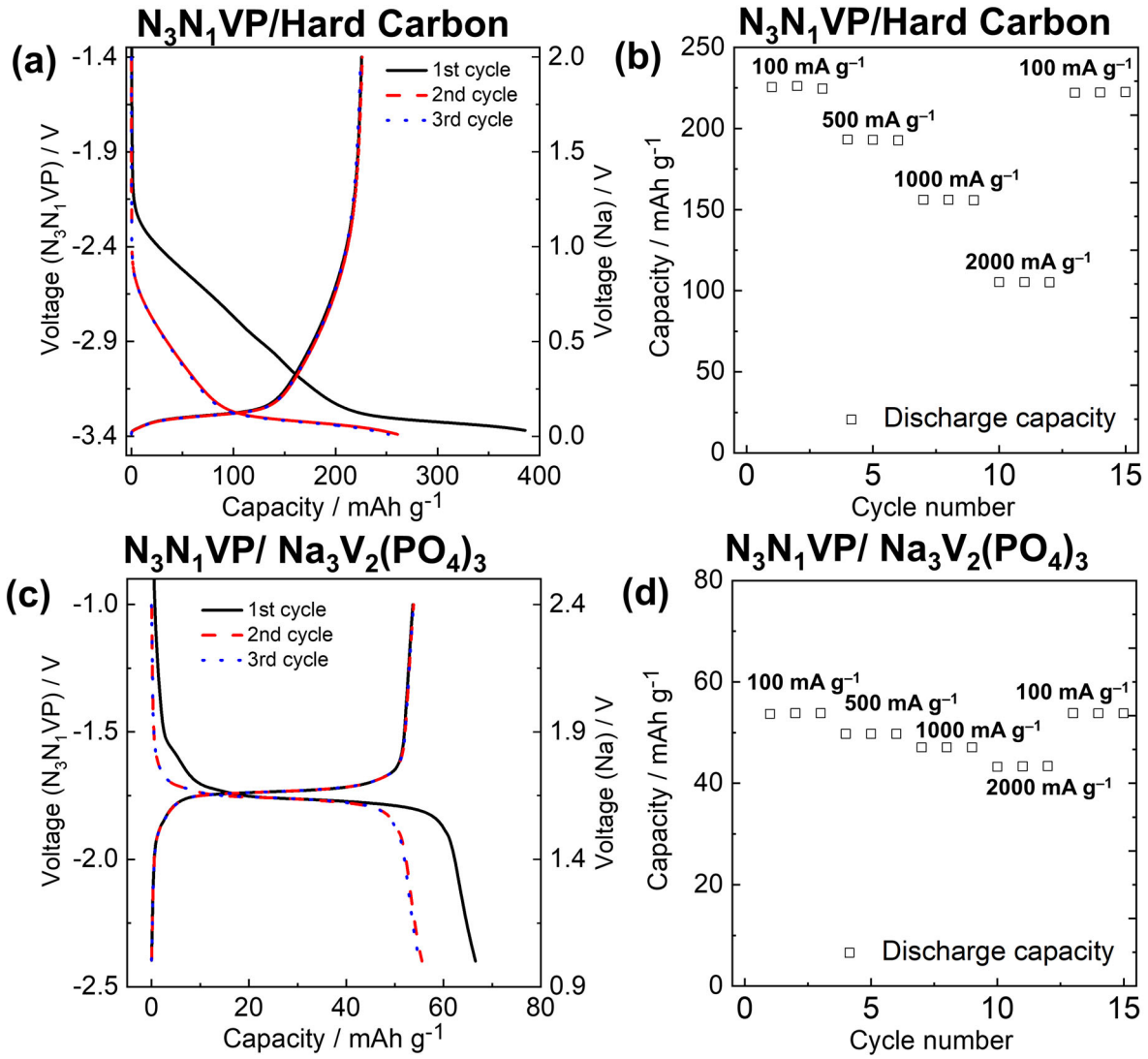

Fig. S17 Negative electrodes tests using the N_3N_1VP counter electrode at 25 ºC. a) Charge-discharge curves of the N_3N_1VP/OE/Hard carbon cell, b) rate capability of the N_3N_1VP/OE/Hard carbon cell, c) charge-discharge curves of the N_3N_1VP/OE/$Na_3V_2(PO_4)_3$ cell and d) rate capability of the N_3N_1VP/OE/$Na_3V_2(PO_4)_3$ cell. Current density: 100 mA g^{-1} for charge-discharge test and 100−2000 mA g^{-1} for rate capability test. Cut-off voltage: –3.39/−1.4 V for the N_3N_1VP/OE/Hard carbon cell and –2.4/−1.0 V for the N_3N_1VP/OE/$Na_3V_2(PO_4)_3$ cell.

References

1. Z. Jian, C. Yuan, W. Han, X. Lu, L. Gu, X. Xi, Y.-S. Hu, H. Li, W. Chen, D. Chen, Y. Ikuhara and L. Chen, *Adv. Funct. Mater.*, 2014, **24**, 4265-4272.
2. J. Hwang, K. Matsumoto and R. Hagiwara, *Adv. Sustainable Syst.*, 2018, **2**, 1700171.
3. J. Hwang, K. Matsumoto and R. Hagiwara, *ACS Appl. Energy Mater.*, 2019, **2**, 2818-2827.
4. R. Dugas, A. Ponrouch, G. Gachot, R. David, M. R. Palacin and J. M. Tarascon, *J. Electrochem. Soc.*, 2016, **163**, A2333-A2339.
5. J. Rodríguez-Carvajal, *Phys. B*, 1993, **192**, 55-69.
6. K. Momma and F. Izumi, *J. Appl. Crystallogr.*, 2008, **41**, 653-658.